

# FINE-SCALE VERTICAL STRUCTURE OF A COLD FRONT AS REVEALED BY AIRBORNE 95 GHZ RADAR

Bart Geerts<sup>1</sup> and Dave Leon  
University of Wyoming

## 1. INTRODUCTION

In the afternoon of 24 May 2002 a vigorous cold front moved through the Texas Panhandle. The front was intercepted by an armada of mobile observing platforms as part of the International Water Vapor Project (IHOP, Weckwerth et al 2003). The objective of the mission was to capture the initiation of thunderstorms in an area marked by a well-defined dryline and a protruding cold front. The focus on this paper is on the fine-scale vertical structure of this cold front documented, using aircraft in situ measurements and data from the Wyoming Cloud Radar (WCR) – an airborne Doppler radar.

This (WCR), is a 95 GHz (3 mm), dual-channel, Doppler radar. The WCR was installed onboard the Wyoming KingAir (UWKA) aircraft in an installation using zenith, nadir, and downward-slanted beams. The WCR was operated mainly in one of two dual-beam modes. The first, profiling mode, uses both the nadir and zenith beams simultaneously. The second mode uses the nadir beam in conjunction with the second, downward-slanted beam (slanted 30° forward of nadir). The profiling mode allows near-vertical velocities to be measured within 100-125m above and below the aircraft, while the second mode, referred to as the VPDD (vertical plane dual-Doppler) mode, allows vertical and horizontal (along-track) velocity components to be retrieved. For both modes, the resolution is 30m or better for the ranges and pulse widths used here.

It has long been postulated that, on the meso- $\gamma$  scale, the cold air associated with a cold front may assume the vertical structure of a density (or gravity) current. Such current results when two fluids of different density are juxtaposed. Due to gravity, the denser fluid will penetrate below the less dense fluid in the form of a shallow current with an elevated head and turbulent wake. Atmospheric density currents have received a great deal of attention (Simpson 1987) and have been invoked in the interpretation of thunderstorm-generated gust fronts, sea breezes, land breezes, katabatic winds spreading over level terrain, as well as cold fronts (e.g. Wakimoto and Bosart 2000). The fine structure of density currents is well known from laboratory experiments (e.g. Simpson and Britter 1980), however *the existence of such structure in the atmosphere has only been inferred*, because observations are generally too coarse in resolution.

The cold front and its environment were largely free of cloud, however (optically) clear-air returns were sufficiently strong for the WCR to measure reflectivity

and Doppler velocity in the region of the front. During the warm season, cold-frontal density currents and other convergence lines are often apparent as a “fine-lines” on the base reflectivity displays of WSR-88D radars, at least within a limited range, e.g. 60 km. This suggests that they are confined to the boundary layer or its top. Forecasters have come to monitor these fine-lines as loci of possible convective initiation. At X, C and S-band, and a fortiori at mm wavelengths, these clear-air echoes are dominated by insects (Russell and Wilson 1997).

## 2. AIRBORNE W-BAND VELOCITY PROCESSING – DUAL-DOPPLER ANALYSIS

During IHOP the WCR operated in VPDD mode for flight legs above 700 m AGL, while for flight levels below 700 m AGL the profiling mode was used (for the lowest flight levels only the zenith beam was used). For straight flight legs using the VPDD mode the nadir-beam re-samples the same volume observed by the downward-slanted beam after a short delay (~6 sec per km below the aircraft). The two Doppler velocity measurements can be combined to give horizontal and vertical velocity components arranged in a vertical-plane below the aircraft – the VPDD synthesis.

During IHOP the WCR used a 225 ns pulse along with a prf of 20 kHz resulting in a range resolution of ~30m and an unambiguous velocity width of 31.6 ms<sup>-1</sup>. The minimum detectable signal at 1km range is ~ -28 dBZ. The first gate with reliable velocities is 120 meters below the aircraft. The radial velocities for each beam are corrected for the effects of platform motion using INS/GPS measurements of aircraft velocity and attitude.

The WCR echoes are believed to be dominated by small insects, which exist at much higher concentrations in the convective boundary layer CBL than larger insects, especially above the lowest 100 m (Vaughn 1985). Because essentially all insects fall within the Mie regime at W-band the scattering depends less on the size of the scatterers than would be the case for Rayleigh scatterers. Therefore, and because larger insects exist in smaller numbers, small insects should dominate the echoes. This is important for velocity retrievals since small insects do not migrate, causing no bias in the retrieved horizontal velocity. However it seems likely that insects tend to oppose the updraft in which they become embedded. It is the only convincing explanation for the existence and persistence of fine lines, where the echo strength is some 10-30 dB above background values, implying insect concentrations 1-3 orders of magnitude higher than background values (the concentration of purely passive tracers would not be altered by convergence features).

Vertical Doppler velocities in the zenith and nadir beams (using the closest reliable gates to the aircraft)

<sup>1</sup> Corresponding author address: Dr. Bart Geerts, Dept of Atmospheric Science, University of Wyoming, Laramie WY 82071, USA; email: geerts@uwyo.edu

have been compared to vertical air motions measured using the WKA gust probe. This comparison has been carried out on several hours of flight legs through the undisturbed CBL, far away from cold fronts or other radar fine-lines. This assessment shows a systematic negative bias in the WCR vertical velocities compared to the gust-probe vertical air velocity (see the companion paper by Geerts and Miao in this Preprint Volume). This bias, about  $0.55 \text{ ms}^{-1}$  on average, is larger in stronger updrafts, e.g. in a  $4 \text{ m s}^{-1}$  updraft the bias is about  $2.3 \text{ m s}^{-1}$ . A constant correction of  $0.5 \text{ ms}^{-1}$  has been added to the vertical Doppler velocities so that they approximate the vertical air velocities. However, the contamination due to the motion of the scatterers remains the largest source on uncertainty in the vertical velocities.

### 3. MESOSCALE ENVIRONMENT

In the afternoon of May 24 2002, a SW-NE oriented cold front approached a nearly stationary, north-south oriented dryline (Weckwerth et al 2003) (Fig 1). This front was not very strong in the morning hours, but frontogenesis occurred during the daytime as the cold sector remained covered by a vast stratus deck (Trudel 2003). At 12 UTC, the surface temperature difference between Guymon OK on the cold side of the front and Childress TX, some 270 km south on the warm side, was 6 K. Six hours later it was 21 K, due solely to warming at Childress.

The cold front was mostly stationary and ill-defined in the morning hours (10-14 UTC), but it accelerated thereafter. The base reflectivity display of the Amarillo WSR-88D did not capture the cold front as a convergent fine-line until 20:00 UTC, about 4 hours *after* passage at the radar site. Similarly, radar and surface station data do not reveal a dryline until about 19:30 UTC. Indeed fine-line development did not occur until several hours after the development of the CBL.

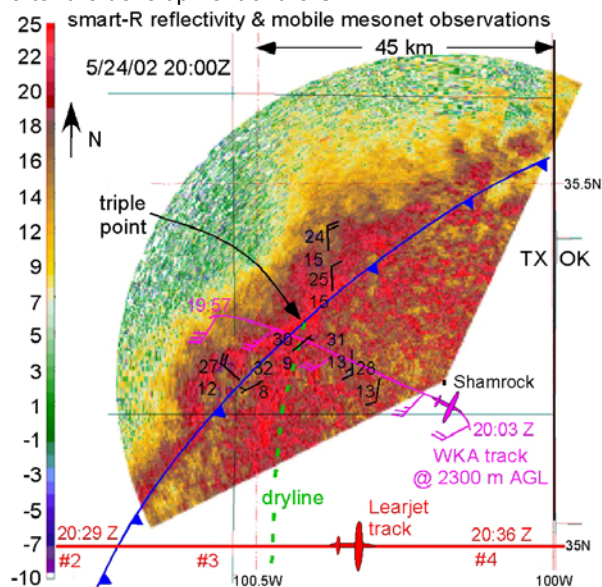


**Fig 1.** SMART-R 0.5 degree elevation reflectivity scan, plus mobile mesonet observations, at 20:00 UTC, in the Texas Panhandle just west of the Oklahoma border.

Also shown are the WKA track, nearly intersecting the triple point, with flight-level winds at 700 mb, and the Learjet track, with the location of dropsondes shown in Fig 2.

Deep convection broke out along the SSW-NNE oriented dryline, first around 20:10 UTC, near Childress, about 90 km south of Shamrock (Fig 1). Later the convection progressed northward, with the first towering cumulus along the cold front at 21:20 UTC. Several severe thunderstorms ensued along the cold front in the following hours.

Eight sondes were dropped around 20:30 UTC from 4700 m MSL along an east-west leg located north of the WKA flight tracks (Fig 2). In the eastern half of this leg, a deep mixed layer exists with mixing ratio values around  $12 \text{ g kg}^{-1}$ . This layer is weakly capped at about 800 mb, where over a depth of 10 mb, the potential temperature  $\theta$  jumps by about 2 K, the mixing ratio by about  $3 \text{ g kg}^{-1}$ , and the wind shifts from southeasterly to southwesterly.

Dropsonde #3 shows a deeper mixed-layer, about 2.7 km deep, and is drier (mixing ratio  $\sim 9 \text{ g/kg}$ ). Near the top of this deep mixed layer, the sonde suggests that the relative humidity peaks at about 85%, while  $\theta_e$  decreases some 14K between 2.7-3.7 km AGL.

The low-level moisture gradient and confluence between sondes #3 and #4 suggests that a dryline was developing or intensifying there. A 19 UTC aircraft sounding on the moist side of the dryline reveals a CBL about 1.8 km deep, with stratocumulus clouds in the upper 800 m of the CBL, and a mixing ratio of  $\sim 9 \text{ g/kg}$  above the CBL. Smart-R and mobile mesonet data show that the dryline was convergent and intensifying at that time. Soundings #4-#8 have very little CIN and ample CAPE, i.e. this broad region is ready for convective initiation.

The cold front, propagating at increasing speed, and the developing dryline intersected near Shamrock (Fig 1). The triple point became the focus of intensive observations. The WKA flew multiple legs, 30-50 km long, from 150 m to 2440 m above ground level (AGL) crossing both the dryline and cold front.

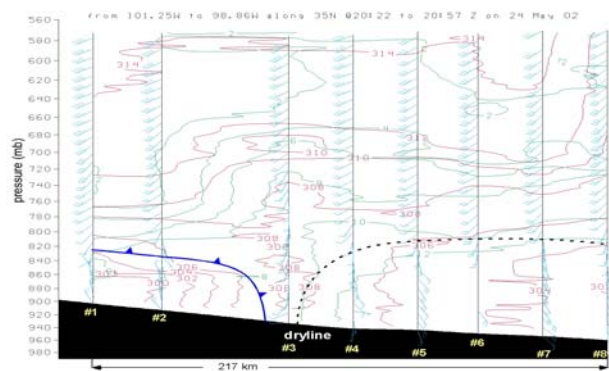


**Fig 2.** Cross section across the cold front and dryline, based on a series of dropsondes. This section runs west to east across the Texas Panhandle (Fig 1). Sondes were dropped between 20:22-20:57 UTC. Mixing ratio is shown in green ( $\text{g kg}^{-1}$ ),  $\theta$  (K) in red.

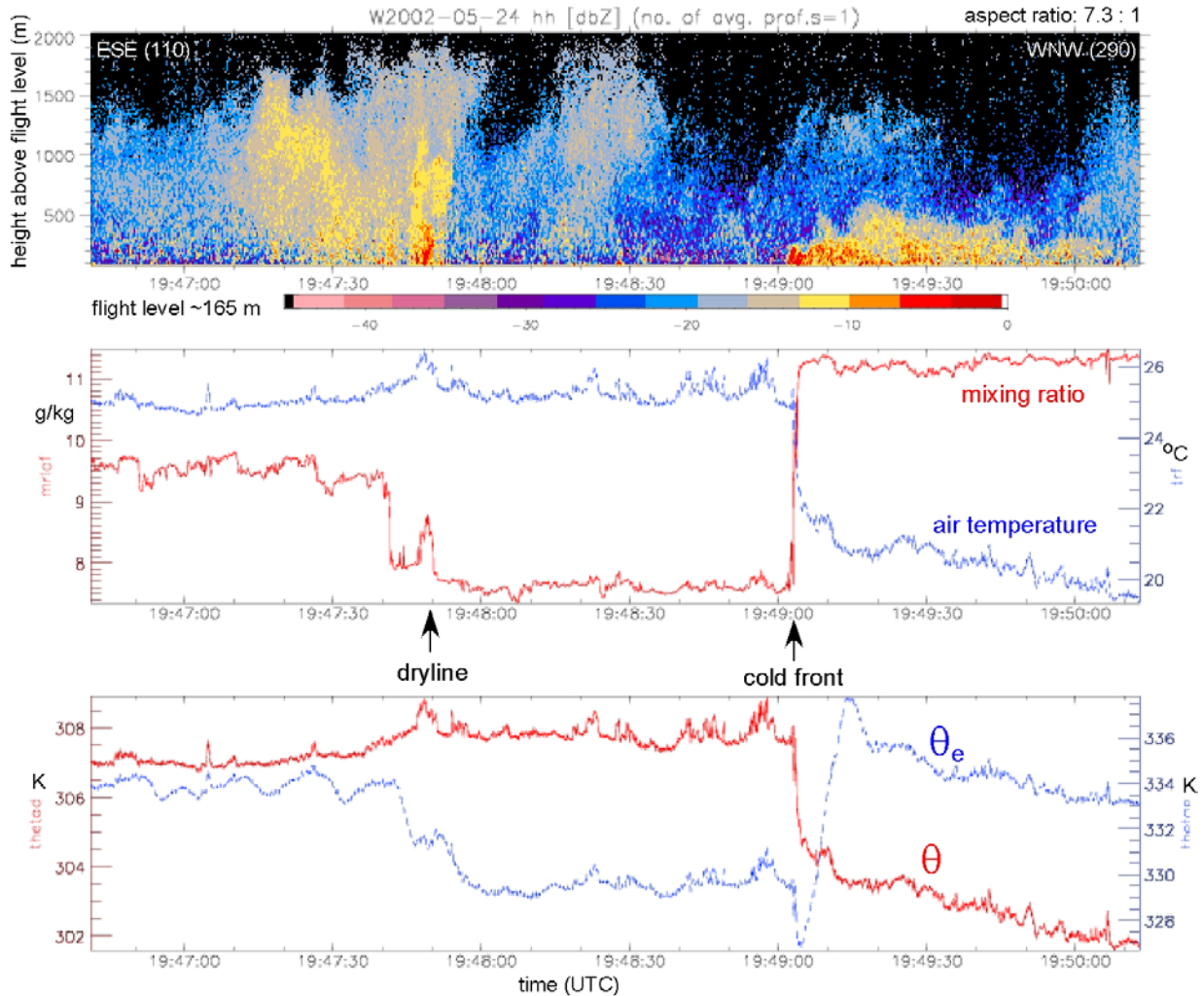


**Fig 3.** (top panel) WCR reflectivity profile above flight level, along a 22 km long transect from ESE to WNW on 24 May 2002 in northern Texas, displayed at an aspect ratio of 2.5:1; (middle panel) flight-level data below the WCR transect, with mixing ratio (thick line) and air temperature (thin line); (bottom panel) ibidem, but (equivalent) potential temperature in (thin) thick line.

#### 4. AIRCRAFT AND RADAR TRANSECTS

The WKA crossed the cold front ten times during a two-hour period (19:07-21:14 UTC), which witnessed the protrusion of the cold front into the moist air east of the dryline, and the eruption of deep convection to the south and east of the cold front. WCR reflectivity (up-looking) and corresponding in situ measurements for a low level transect of the cold front/dryline are shown in **Fig. 3**. The vertical echo structure of the quasi-stationary dryline, about 1600 m deep, stands in marked contrast to the rearward-sloping frontal boundary, which was only ~500 m deep and propagated at 6-7  $\text{ms}^{-1}$ . The greater depth of the dryline explains why it could be seen at greater range than the cold front on WSR-88D radar, at least in this case. Much remains to be explored regarding the vertical structure of radar fine lines.

The WCR reflectivity transect shown in Fig 3 does not discriminate between clear-air and cloud echoes in the moist side of the dryline. Visible satellite and surveillance radar imagery reveal cloud/echo streets, evidence of horizontal convective rolls, east of the dryline. The dryline itself is evident as an enhanced echo plume, some 2 km deep. The dry sector, with  $\sim 2 \text{ g kg}^{-1}$  less moisture and a slightly higher temperature ( $< 1\text{K}$ ), is cloud-free. The cold front is very sharp, with a 3 K temperature drop in less than 100 m and continued temperature drop beyond.

The postfrontal air is *more* humid than the moist air ahead of the dryline (Fig 3), and indeed, a few kilometers northwest of the surface cold front, the shallow cold-frontal surface was capped by a stratus cloud deck. The result is that while  $\theta$  is lower behind the cold front, the  $\theta_e$  is actually *higher* within the leading edge of the cold air. Flight-level  $\theta_e$  values are 7 K higher in the leading edge of the cold air than in

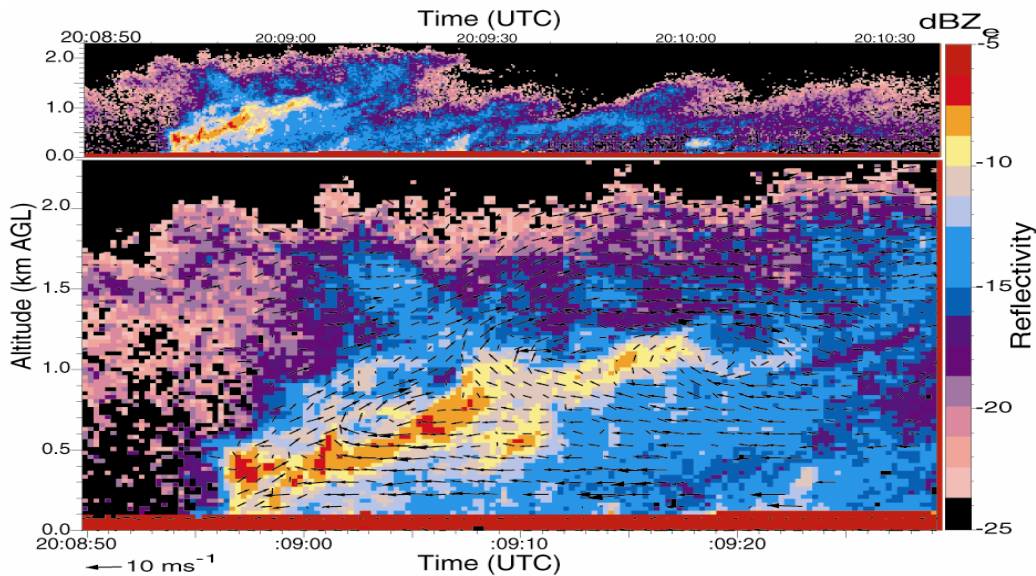


**FIG 4.** Reflectivity and velocity vectors for a transect across the cold front. Aspect ratio for both images is 1:1. The lower image is a zoom-in of the upper one.

the dry sector and some 3 K higher than that in the plume that marks the dryline, and further east. Dropsonde data (Fig 2) do not resolve this local maximum in  $\theta_e$ , but they do capture the decrease in  $\theta_e$  deeper in the cold air.

In the next 20 minutes, the cold front penetrated into the moist air, lifting the dryline echoes. A cross-section of VPDD-derived air motion across the cold front, some 20 minutes later than the transect shown in Fig 3, is shown in Fig 4. A SMART-R reflectivity overlay indicates that this transect is across the triple point. The vectors shown in Fig 4 are undersampled, the true grid spacing is 30 m. The updraft above the leading edge of the front is consistent with low-level convergence in the plane of this transect. Strong wind shear, about  $20 \text{ ms}^{-1}$  vertically across the frontal surface, resulted in the breakdown of the horizontal interface between the warm and cold air through a series of large-amplitude Kelvin-Helmholtz billows. It is remarkable to see in this and other transects that vortices form on the leading edge (the density current itself). Presumably they amplify as they are advected rearward, in one case leading to up-and downdraft cores peaking at  $8 \text{ ms}^{-1}$ , separated by just 600 m.

Breaking waves on the frontal surface have also been observed on the surface of laboratory density currents. Other characteristics consistent with a density current include a well-defined, but highly variable head, front-relative rear-to-front flow within, and the presence of clefts and lobes (not shown).

## 5. CONCLUSIONS

The fine-scale vertical structure of a strong cold front is elucidated by means of aircraft observations and high-resolution ( $\sim 30 \text{ m}$ ) Doppler radar observations. The front intersected with a dryline and deep convection was initiated, first along the dryline.

The fine-scale cold-frontal circulation bears many similarities to that of a density current. In particular, Kelvin-Helmholtz billows are present in all ten transects. Cores of high horizontal vorticity appear at the density current head, and these may be precursors to the trailing K-H billows.

A more in-depth analysis is under way.

*Acknowledgements:* This research is supported by National Science Foundation grant # ATMS0129374. Tim Trudel aided in the mesoscale analysis, and Sam Haimov coordinated the WCR data collection in IHOP. Rick Damiani provided Fig 3.

## REFERENCES

- Russell, R.W., and J.W. Wilson, 1997: Radar-observed "fine lines" in the optically clear boundary layer. Reflectivity contributions from aerial plankton and its predators. *Bound-Layer Met.*, **82**, 235-262.
- Simpson, J.E., 1987: *Gravity Currents: In the Environment and the Laboratory*. Ellis Horwood Ltd. Publ., 244 pp.
- \_\_\_\_\_, and Britter, R.E. 1980: A laboratory model of an atmospheric mesofront. *Quart. J. Roy. Meteor. Soc.*, **106**, 485-500.
- Trudel, T., 2003: Convective initiation near a cold front-dryline triple point: the IHOP 5/24/02 case. MS thesis, University of Wyoming, to be submitted in summer 03.
- Vaughn, C.R., 1985: Birds and insects as radar targets: a review. *Proc. IEEE*, **73**, 205-227.
- Wakimoto, R.M., and B.L. Bosart, 2000: Airborne radar observations of a cold front during FASTEX. *Mon. Wea. Rev.*, **128**, 2447-2470.
- Weckwerth, T. M., and co-authors, 2003: An overview of the International H<sub>2</sub>O Project (IHOP\_2002) and some preliminary highlights. Submitted to the *Bull. Amer. Meteor. Soc.*